

10,11

# One-dimensional carbon structures formed on transition metal oxides

© S.Yu. Davydov

Ioffe Institute,  
St. Petersburg, Russia  
E-mail: sergei\_davydov@mail.ru

Received November 25, 2024

Revised December 16, 2024

Accepted December 17, 2024

We consider epitaxial cumulene as a carbon chain formed in a groove on a transition metal oxide (TMO) face. A simple model of the density of states of TMO is proposed. A model of a one-dimensional analogue of graphene oxide (1DGO) has been constructed, which is a decorated cumulene, every second atom of which is bonded to an oxygen atom ( $C_2O$ ). It has been shown that decoration leads to the opening of a gap in the electronic spectrum. Estimates of the influence of the TMO substrate ( $TiO_2$ ) on the spectral characteristics, effective masses, and densities of states of cumulene and 1DGO are presented.

**Keywords:** cumulene, transition metal oxides, graphene oxide, electron spectrum.

DOI: 10.61011/PSS.2025.01.60600.321

## 1. Introduction

The advent of graphene materials triggered the search for new two-dimensional (2D) compounds [1–5]. Interest in one-dimensional (1D) structures has also increased: see references in Refs. [6–8], where analytical expressions for dispersion, effective carrier masses, and densities of free carbines were obtained in the strong coupling approximation [6,7], and also discussed the experimental and theoretical prerequisites for the creation of long carbon chains on grooved faces of d-metals [8]. Here, a similar problem is considered for substrates representing transition metal oxides (TMO) [9–17], the grooved faces of which [9,10], as in the case of d-metals [8], presumably should contribute to the formation of one- and quasi-one-dimensional epitaxial structures. It should be emphasized that TMO were chosen as a substrate not only because of the crystallographic specificity of the faces, but also because of the peculiarities of their electronic structure: the energy differences between  $d^n$ - and  $d^{n\pm 1}$ -electron configurations are small in TMO [9,10]. As a result, many transition metals form a whole set of oxides: for example, for vanadium we have VO,  $V_2O_3$ ,  $VO_2$ ,  $V_2O_5$ , where the charge of vanadium atoms is formally equal to +2, +3, +4 and +5. Intermediate valence states are also possible, since the TMO series has mixed states and nonstoichiometric phases of variable composition [9,10].

The band structure of semiconductor TMO is a valence band formed predominantly by 2p-states of oxygen, separated by a band gap from the conduction band formed by TM (d- and valence s-states) [9,10], which can be quite narrow (especially for 3d-oxides), so ignoring the electron-electron and electron-phonon interactions are not always acceptable. Accounting for the first of these interactions requires the introduction of Hubbard electron repulsion, which, for example, leads to a magnetic insulator state

for NiO, accounting for the second makes it necessary to introduce the concept of a polaron. High-temperature superconductors  $La_{1.85}Sr_{0.15}CuO_4$  and  $YBa_2Cu_3O_{7-x}$  should also be mentioned. Thus, TMO substrates represent a promising platform for the formation of epitaxial 1D structures, the properties of which, due to the proximity effect, may significantly differ from their properties in the free state. The standard cumulene as a seed structure and decorated cumulene where every second atom of the carbon chain is connected to an oxygen atom considered as a one-dimensional analog of graphene oxide are considered as epitaxial layers.

## 2. Electronic spectrum of epitaxial carbon chains

### 2.1. General ratios

Let us use the adsorption approach to describe the effect of the substrate on the electronic spectrum of the epitaxial structure [8,18]: if the Green's function of the free structure is  $G(\omega, \mathbf{k}) = (\omega - \varepsilon(\mathbf{k}) + i0^+)^{-1}$ , where  $\varepsilon(\mathbf{k})$  is the dispersion law,  $\mathbf{k}$  is the wave vector, then the Green's function of the epistructure  $\tilde{G}(\omega, \mathbf{k})$  is determined by the Dyson equation  $\tilde{G}^{-1}(\omega, \mathbf{k}) = G^{-1}(\omega, \mathbf{k}) - \Sigma(\omega)$ . The self-energy in this equation is  $\Sigma(\omega) = \Lambda(\omega) - i\Gamma(\omega)$ , where the functions of broadening and shifting the energy levels of the free structure are equal, respectively

$$\Gamma(\omega) = \pi V^2 \rho_{\text{sub}}(\omega), \quad \Lambda(\omega) = \pi^{-1} P \int_{-\infty}^{\infty} \frac{\Gamma(\omega') d\omega'}{\omega - \omega'}, \quad (1)$$

$V$  is the matrix element of interaction of free structure states with substrate states,  $\rho_{\text{sub}}(\omega)$  is the density of substrate states,  $P$  is the symbol of the principal integral value. Thus,

for further analysis, it is necessary to define an expression for the density of states of the TMO substrate  $\rho_{\text{TMO}}(\omega)$ , where  $\omega$  is the energy. Based on the results of numerical calculations [9–17], performed using various variants of the density functional theory (DFT), we represent  $\rho_{\text{TMO}}(\omega)$  as the sum of the densities of states of the valence band  $\rho_V(\omega)$  and the conduction band  $\rho_C(\omega)$ :

$$\rho_{\text{TMO}}(\omega) = \rho_V(\omega) + \rho_C(\omega). \quad (2)$$

Since, according to [9–17], the band is formed by oxygen  $p$ -states, and the conduction band is formed by TM  $d$ -states, let's assume that

$$\rho_{V,C}(\Omega_{V,C}) = \begin{cases} \bar{\rho}_{V,C}, & |\Omega_{V,C}| \leq W_{V,C}/2, \\ 0, & |\Omega_{V,C}| > W_{V,C}/2. \end{cases} \quad (3)$$

Here  $\bar{\rho}_{V,C}$  is the constant,  $\Omega_{V,C} = \omega - \bar{\omega}_{V,C}$ ,  $\bar{\omega}_{V,C}$  is the energy of the center of the valence band/conduction band,  $W_{V,C}$  is the width of the valence band/conduction bands. Then  $\bar{\omega}_C - \bar{\omega}_V = E_g + (W_V + W_C)/2$ , where  $E_g$  is the width of the TMO band gap. Expressions (2) and (3) are a combination of Haldane-Anderson models for semiconductors [19,20] and Friedel models for TM [8,21]. Since  $\bar{\Gamma}_{V,C} = \pi \bar{\rho}_{V,C} V_{V,C}^2$ , where  $V_{V,C}$  is the matrix element of the interaction of the electronic states of the 1D structure and the states of the valence band/conduction band of TMO, we obtain from (1) and (2)

$$\Lambda_{\text{TMO}}(\omega) = \Lambda_V(\omega) + \Lambda_C(\omega), \quad (4)$$

$$\Lambda_{V,C}(\Omega_{V,C}) = \frac{\bar{\Gamma}_{V,C}}{\pi} \ln \left| \frac{\Omega_{V,C} + W_{V,C}/2}{\Omega_{V,C} - W_{V,C}/2} \right|. \quad (5)$$

A nonmagnetic TM was considered in expressions (2)–(5), a generalization of the Friedel model for the presence of TM magnetization is given in Ref. [21]. In this case, we need to represent the density of states of the conduction band formed by TM  $d$ -states as  $\rho_C(\omega) = \sum_{\sigma} \rho_C^{\sigma}(\omega)$ , where  $\sigma = (\uparrow, \downarrow)$  is the spin index,  $\rho_C^{\sigma}(\omega) = \bar{\rho}_C/2$  for  $|\Omega_C^{\sigma}| \leq W_C/2$  and  $\rho_C^{\sigma}(\omega) = 0$  at  $|\Omega_C^{\sigma}| > W_C/2$ ,  $\Omega_C^{\sigma} = \omega - \bar{\omega}_C^{\sigma}$ ,  $\bar{\omega}_C^{\sigma}$  is the energy of the center of  $\sigma$ -subband of the conduction band. Then we obtain  $\bar{\Gamma}_C^{\sigma} = \bar{\Gamma}_C/2$  and  $\Lambda_C(\omega) = \sum_{\sigma} \Lambda_C^{\sigma}(\omega)$ . Thus, the initially nonmagnetic structure acquires magnetization in the epitaxial state (proximity effect).

## 2.2. Estimates of model parameters

Let's assume that  $\bar{\rho}_V = 6/W_V$  and  $\bar{\rho}_C = 10/W_C$ , where 6 and 10 are the numbers of  $p$ - and  $d$ -states,  $W_{V,C}$  is the width of the valence band/conduction band. According to experimental and numerical calculations for 3d monoxides, we have  $E_g \approx 2\text{--}4\text{ eV}$ ,  $W_V \approx 8\text{ eV}$  and  $W_C \approx 2\text{--}3\text{ eV}$  [11–13]. Then  $\bar{\rho}_V \approx 0.75\text{ eV}^{-1}$ ,  $\bar{\rho}_C \approx 4\text{ eV}^{-1}$ . Let us now estimate the values of the matrix elements  $V_{V,C}$  using the Harrison formulas [22–24]. Understanding  $V_V$  as the matrix element of  $\sigma$ -bonds of the  $p$ -states of carbon and oxygen atoms,

let us assume  $V_V = V_{\text{pp}\sigma} = 2.22 \cdot \hbar^2 / (m_0 \cdot l_{\text{CO}}^2)$ , where  $\hbar$  is the reduced Planck constant,  $m_0$  is the mass of the free electron,  $l_{\text{CO}}$  is the length of bond C–O [23]. The matrix element linking the  $p$ -state of carbon with the  $d$ -state of TM,  $V_C = V_{\text{pd}\sigma} = 2.95 \cdot \hbar^2 r_d^{3/2} / (m_0 \cdot l_{\text{CTM}}^{7/2})$ , where  $r_d$  is the radius of the  $d$ -shell ( $\sim 1\text{ \AA}$  [22]),  $l_{\text{CTM}}$  is the length of the bond C–TM (we use here the formula given in Chapter 19 of Ref. [22] for ordinal estimates of the matrix element, rather than the more complex expression from Ref. [24]). As in Ref. [22], we assume that  $l_{\text{CO}} = r_a(\text{C}) + r_a(\text{O})$  and  $l_{\text{CTM}} = r_a(\text{C}) + r_a(\text{TM})$ , where  $r_a$  is the atomic radius. We obtain  $\bar{\Gamma}_C/\bar{\Gamma}_V \approx 2$  using the values  $r_a$  from Ref. [25] and assuming  $l_{\text{CO}} \approx l_{\text{CTM}} \approx 2\text{ \AA}$  for a rough estimate. The dependences  $\Lambda_V(\omega)$ ,  $\Lambda_C(\omega)$ , and  $\Lambda_{\text{TMO}}(\omega)$  for the nonmagnetic case are shown in Figure 1. It should be noted that the shift and broadening of the states of 1D structures in the case of a TM substrate are determined by the functions  $\Lambda_C(\omega)$  and  $\Gamma_C(\omega)$ , which describe the effect of the  $d$ -band of the transition metal conductivity.

## 3. Cumulene decorated with oxygen atoms as a 1D analog of graphene oxide

A number of free one-dimensional structures were considered in Ref. [8]: monatomic and diatomic chains and the quasi-one-dimensional structure  $ABC$ . We consider in this paper the 1D analog of the two-dimensional graphene oxide 2DGO [26–29], or 1DGO. We would like to remind that 2DGO has the graphene structure, but contains oxygen (C–O–C, C=O) and/or functional groups of the type (–OH, –COOH). As a basis for simulation, let's take the Hoffmann structural model of two-dimensional graphene oxide (GO) (corresponding to the chemical formula  $\text{C}_2\text{O}$ ), for which the structure  $ABC$  is suitable (see Figure 1 in [8]), where the atoms  $A$  and  $B$  denote carbon, and the atoms  $C$  denote oxygen. 1DGO can be considered as a decorated cumulene, where every second carbon atom is bound to an oxygen atom.

Using the formula (5) from [8] and introducing the notation  $\varepsilon_A = \varepsilon_B = \varepsilon(\text{C}) = \varepsilon$ ,  $\varepsilon_C = \varepsilon(\text{O}) = \varepsilon - \delta$ ,  $\Omega = \omega - \varepsilon$ , we obtain the equation

$$(\Omega + \delta)[\Omega^2 - 4t^2 \cos^2(ka)] - \Omega t_{\perp}^2 = 0, \quad (6)$$

the roots of which determine the dispersion of electrons in 1DGO. It is useful to further consider three special cases:

$$\left. \begin{aligned} 1) & \text{ if } t_{\perp} = 0 \text{ we have } \omega_0 = -\delta \\ & \text{ and } \omega_{\pm} = \pm 2t \cos(ka) \text{ (cumulene);} \\ 2) & \text{ if } t = 0 \text{ we have } \omega_0 = 0 \\ & \text{ and } \omega_{\pm} = -\delta \pm \sqrt{\delta^2 + 4t_{\perp}^2}/2 \text{ (CO dimer);} \\ 3) & \text{ if } \delta = 0 \text{ we have } \omega_0 = 0 \\ & \text{ and } \omega_{\pm} = \pm 2t \sqrt{\cos^2(ka) + t_{\perp}^2/t^2}. \end{aligned} \right\} \quad (7)$$

Proceeding to the solution of equation (6), we would like to note, first, that the atomic radii of carbon and oxygen are almost the same [25] (as well as the lengths of bonds C–C and C–O), so that  $t \approx t_\perp$  and  $t \approx 2.8\text{--}3\text{ eV}$  [6,7,30,31].

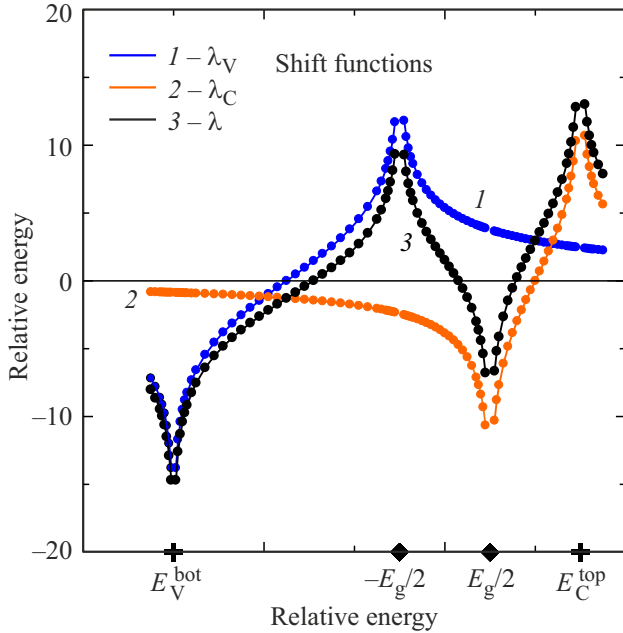


**Figure 1.** Functions of the shift caused by the valence band  $\Lambda_V(\omega)$  (curve 1) and conduction band  $\Lambda_C(\omega)$  (2) and their sum  $\Lambda_{TMO}(\omega)$  (3);  $E_V^{\text{bot}}$  and  $E_C^{\text{top}}$  are the energies of the bottom and ceiling of the valence band and the conduction band. The zone of valence s-states lying above  $E_C^{\text{top}}$  is not shown in the figure. The value of  $E_g/2 = 1.5\text{ eV}$  is taken as a unit of energy:  $W_V = 5$ ,  $W_C = 2$ ,  $\bar{\Gamma}_V = 3.0$ ,  $\bar{\omega}_V = -3.5$ ,  $\bar{\Gamma}_C = 3.5$ ,  $\bar{\omega}_C = 2$ .

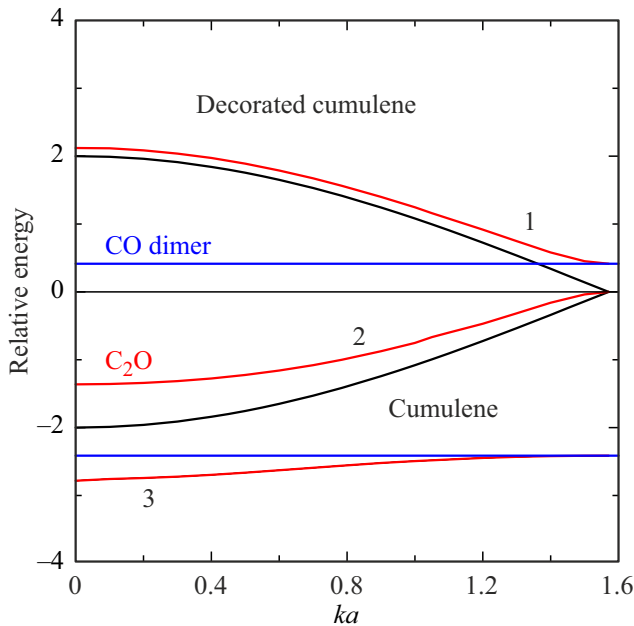


**Figure 2.** Zones of decorated cumulene  $C_2O$   $\omega_i(k)$ , where  $i = 1, 2, 3$  (shown by red color), and CO dimer levels (shown by blue color):  $\varepsilon = 0$ ,  $t = t_\perp = 1$  and  $\delta = 2$ .

According to the tables of Mann atomic terms [23], we obtain  $\delta = 5.7\text{ eV}$ , which allows us to assume  $\delta = 2t$ . The dependencies  $\omega_i(k)$  obtained from solving the equation (6) are shown in Figure 2. The widths of the bands are equal:  $W_1 \approx 1.71t$ ,  $W_2 \approx 1.41t$ ,  $W_3 \approx 0.37t$ ; the width of the gap at the border of the Brillouin band is  $\Delta = 0.41t$ . We obtain the following in the limit  $qa \ll 1$  by introducing the wave vector  $q = \pi/(2a) - k$  and assuming  $\varepsilon = 0$

$$\varepsilon_{1,3}(q) = \bar{\varepsilon}_{1,3} + v_{1,3}(q), \quad \varepsilon_2(q) = -(4t^2\delta/t_\perp^2)(qa)^2, \quad (8)$$

$$\bar{\varepsilon}_{1,3} = \delta[-1 \pm \sqrt{1 + 4t_\perp^2/\delta^2}]/2,$$

$$v_{1,3}(q) = \frac{4t^2(\bar{\varepsilon}_{1,3} - \delta)}{3\bar{\varepsilon}_{1,3}^2 - 2\bar{\varepsilon}_{1,3}\delta - t_\perp^2}, \quad (9)$$

where  $\bar{\varepsilon}_1 = (-\delta + \sqrt{\delta^2 + 4t_\perp^2})/2$ ,  $\bar{\varepsilon}_2 = 0$ ,  $\bar{\varepsilon}_3 = (-\delta - \sqrt{\delta^2 + 4t_\perp^2})/2$ . The effective masses are  $m_{1,3} = \hbar^2(3\bar{\varepsilon}_{1,3}^2 - 2\bar{\varepsilon}_{1,3} - t_\perp^2)/[8t^2a^2\bar{\varepsilon}_{1,3} - \delta]$  and  $m_2 = \hbar^2t_\perp^2/(8t^2a^2\delta)$ ; we obtain  $m_{1,2}^* = m^* \approx 0.1$  and  $m_3^* \approx 1.2$  for dimensionless effective masses  $m^* = m/m_e$ , where  $m_e$  is the mass of a free electron, where we assume  $a = 1.28\text{ \AA}$ , which corresponds to the interatomic distance in cumulene [6,7]. Then, in the two-band approximation, the 1DGO spectrum can be represented as  $E_{V,C}(q) = E_g/2 \pm \hbar^2q^2/(2m^*m_e)$ , where  $E_g = 0.41t$ . It is easy to show that for  $\omega \rightarrow \bar{\varepsilon}_i$ , the densities of states corresponding to the branches of the spectrum  $\varepsilon_i(q)$  have the form

$$\rho_i(\omega) = \frac{a\sqrt{|m_i|^2}}{\hbar\sqrt{|\bar{\varepsilon}_i - \omega|}} \quad (10)$$

for  $\omega > \bar{\varepsilon}_1$ ,  $\omega < \bar{\varepsilon}_{2,3}$  and  $\rho_i(\omega) = 0$  in the opposite cases. We would like to underline that the root features of the density of states are characteristic of all one-dimensional structures considered in Ref. [8].

It should be noted that the decoration of carbon 1D chains with oxygen atoms of the TMO substrate seems quite likely and natural, since all oxides exhibit nonstoichiometry associated with oxygen deficiency (i.e., with the loss of some oxygen atoms). Therefore, here we can consider 1DGO both as a free and as a kind of epitaxial structure.

#### 4. Cumulene and 1DGO on the surface of $TiO_2$ (simple estimates)

It follows from the comparison of the Green's functions  $G(\omega, \mathbf{k})$  and  $\tilde{G}(\omega, \mathbf{k})$  that the energy  $\omega$  should be replaced by  $\tilde{\omega} = \omega - \Lambda(\omega)$  [6–8]. Then, instead of the effective masses of the free chains  $m$ , we obtain the masses  $\tilde{m}$ , determined by the ratio

$$\tilde{m}/m = F(\omega_{\text{ext}}), \quad F(\omega) = (1 - d\Lambda(\omega)/d\omega)_{\omega_{\text{ext}}}^{-1}, \quad (11)$$

where  $\omega_{\text{ext}}$  is the energy of the extremum of the band. We obtain from (5)

$$d\Lambda_{V,C}(\omega)/d\omega = \frac{V_{V,C}^2}{\Omega_{V,C}^2 - (W_{V,C}/2)^2}. \quad (12)$$

Thus, if the energy  $\omega_{\text{ext}}$  is in the band gap of the TMO substrate, then  $d\Lambda(\omega)/d\omega < 0$  and  $\tilde{m}/m < 1$ .

The values of the work function for titanium dioxide  $\varphi_{\text{TiO}_2}$  are 4.2–4.3 eV [32], 4.6 eV [33]; the values 5.2–5.8 eV are provided in Ref. [34] for (110)TiO<sub>2</sub>. The variation of values is explained, in most cases, by the nonstoichiometry of TiO<sub>2</sub>. We have  $E_g = 3.2$  eV for (110)TiO<sub>2</sub> [35,36]. Graphene and graphite have the same work functions  $\varphi_{\text{Gr}} = 4.5$  eV [37]; the work functions of monolayer and bilayer graphene also slightly differ (4.6 eV [38]). Therefore, we assume  $\varphi_{\text{cum}} = 4.6$  eV for ordinal estimates. Assuming the work of  $\varphi_{\text{TiO}_2} = \varphi_{\text{cum}} = 4.6$  eV, and assuming that the Dirac point of cumulene  $\varepsilon$  lies at 4.6 eV below the vacuum level, we conclude that the band gap of titanium dioxide is located in the energy range  $(-0.57t, 0.57t)$ , where  $\varepsilon$  is still the beginning of the energy reference. Now it is obvious that the 1DGO gap  $(0, 0.41t)$  is inside the band gap of graphene dioxide (i.e., the 1DGO|TiO interface<sub>2</sub> is a type I heterojunction [39,40]), so we have  $F = \tilde{m}/m < 1$ . The estimates show that for the considered case  $F \approx 0.1$ .

Since the gap in the 1DGO spectrum overlaps with the band gap of TiO<sub>2</sub>, the self-energy transfer  $\Sigma(\omega) = \Lambda(\omega) - i\Gamma(\omega)$  in the expression for the Green's function  $G^{-1}(\omega, \mathbf{k}) = G^{-1}(\omega, \mathbf{k}) - \Sigma(\omega)$  is reduced to  $\Lambda(\omega)$ , since  $\Gamma(\omega) = 0$ . Hence, the density of states  $\tilde{\rho}_i(\omega)$  of 1DGO epitaxial structure is determined by a modified formula (10) of the form

$$\tilde{\rho}_i(\omega) = \frac{a \sqrt{|\tilde{m}_i|/2}}{\hbar \sqrt{|\tilde{\varepsilon}_i - \tilde{\omega}|}}, \quad (13)$$

where  $\tilde{\omega} = \omega - \Lambda(\omega)$  and  $\Lambda(\omega)$  are given by (4) and (5). We would like to underline that the expression (13) is valid only in the energy range  $(0, 0.41t)$ . The same transformation should be applied to the density of states of free cumulene  $\tilde{\rho}_{\text{cum}}^{\pm}(\omega)$  to obtain the density of states of epitaxial cumulene  $\tilde{\rho}_{\text{cum}}^{\pm}(\omega)$  (see formula (11) in [8]).

It should be noted also that under the condition  $\varphi_{\text{sub}} = \varphi_{\text{epi}}$ , there is no charge transfer between the substrate (with work function  $\varphi_{\text{sub}}$ ) and the epitaxial structure (with work function  $\varphi_{\text{epi}}$ ). According to our estimates, this is the case for epitaxial cumulene and 1DGO.

## 5. Concluding remarks

Another feature of TMO that was not noted in the paper is the high values of static permittivity  $\varepsilon_{\text{st}}$ , equal, for example, to 25 for ZrO<sub>2</sub> and HfO<sub>2</sub> and equal to 80 for TiO<sub>2</sub> [41,42]. For comparison: we have  $\varepsilon_{\text{st}} \approx 3.9$  [41] and  $\varepsilon_{\text{st}} \approx 10$  [43] for SiO<sub>2</sub> and SiC, respectively,  $\varepsilon_{\text{st}} \approx 2$ –15 for graphene [31,44]. There is an unprecedented spread of data on static permittivity for GO: the values of  $\varepsilon_{\text{st}}$  from units to  $10^5$  are provided for room temperature and a frequency of 100 Hz [44–46]. Despite the noted uncertainty of the data, the 1DGO|TiO<sub>2</sub> system can be considered as a system with high dielectric susceptibility (high- $\kappa$  system [47]). We

would also like to note the recent increased interest in small-radius polarons in TMO [48–50].

Summing up the results of this work, we would like to note that we proposed (the first, as far as the author knows) a model of one-dimensional cumulene oxide (1DGO) and showed that the addition of oxygen atoms to every second carbon atom leads to the opening of a gap in the electronic spectrum. It is known [26] that the gap width in the 2DGO spectrum depends on the degree of its oxidation and decreases to zero when the last bond C–O is removed. The same effect is observed in our proposed 1DGO model. We propose to further introduce Coulomb and electron-phonon interactions into the 1DGO model according to the diagrams developed in Ref. [6,51,52].

## Conflict of interest

The author declares that he has no conflict of interest.

## References

- [1] J. Nevalaita, P. Koskinen. Phys. Rev. B 97, 3, 035411 (2018).
- [2] S. Haastrup, M. Strange, M. Pandey, T. Deilmann, P.S. Schmidt, N.F. Hinsche, M.N. Gjerding, D. Torelli, P.M. Larsen, A.C. Riis-Jensen, J. Gath, K.W. Jacobsen, J.J. Mortensen, T. Olsen, K.S. Thygesen. 2D Mater. 5, 4, 042002 (2018).
- [3] N. Briggs, S. Subramanian, Z. Lin, X. Li, X. Zhang, K. Zhang, K. Xiao, D. Geohegan, R. Wallace, L.-Q. Chen, M. Terrones, A. Ebrahimi, S. Das, J. Redwing, C. Hinkle, K. Momeni, A. van Duin, V. Crespi, S. Kar, J.A. Robinson. 2D Mater. 6, 2, 022001 (2019).
- [4] L. Vannucci, U. Petralanda, A. Rasmussen, T. Olsen, K.S. Thygesen. J. Appl. Phys. 128, 10, 105101 (2020).
- [5] M. Fukuda, J. Zhang, Y.-T. Lee, T. Ozakia. Mater. Adv. 2, 13, 4392 (2021).
- [6] S.Yu. Davydov. Semiconductors 53, 7, 954 (2019).
- [7] S.Yu. Davydov. Tech. Phys. Lett. 45, 650 (2019).
- [8] S.Yu. Davydov. Phys. Solid State 66, 5, 701 (2024).
- [9] V.E. Henrich, P.A. Cox. The Surface Science of Metal Oxides. Cambridge Univ. Press (1994).
- [10] H.-J. Freund, H. Kühlenbeck, V. Staemmler. Rep. Prog. Phys. 59, 3, 283 (1996).
- [11] R. Gillen, J. Robertson. J. Phys.: Condens. Matter 25, 16, 165502 (2013).
- [12] S. Lany. Phys. Rev. 87, 8, 085112 (2013).
- [13] S. Lany. J. Phys.: Condens. Matter 27, 28, 283203 (2015).
- [14] Y. Guo, L. Ma, K. Mao, M. Ju, Y. Bai, J. Zhao, X.C. Zeng. Nanoscale Horizons 4, 3, 592 (2019). <https://doi.org/10.1039/c8nh00273h>
- [15] W. Li, J. Shi, K.H.L. Zhang, J.L. MacManus-Driscoll. Material Horizons 7, 11, 2832 (2020). <https://doi.org/10.1039/D0MH00899K>
- [16] C. Rdl, F. Fuchs, J. Furthmüller, F. Bechstedt. Phys. Rev. B 79, 23, 235114 (2009).
- [17] E. Engel, R.N. Schmid. Phys. Rev. Lett. 103, 3, 036404 (2009).
- [18] S.Yu. Davydov. Phys. Solid State 58, 4, 804 (2016).
- [19] F.D.M. Haldane, P.W. Anderson. Phys. Rev. B 13, 6, 2553 (1976).

- [20] S.Yu. Davydov, S.V. Troshin. Phys. Solid State **49**, 8, 1583 (2007).
- [21] S.Yu. Davydov. Phys. Solid State **62**, 2, 378 (2020).
- [22] W.A. Harrison. Electronic Structure and the Properties of Solids. W.H. Freeman & Co., San Francisco (1980).
- [23] W.A. Harrison. Phys. Rev. B **27**, 6, 3592 (1983).
- [24] W.A. Harrison, G.K. Straub. Phys. Rev. B **36**, 5, 2695 (1987).
- [25] Fizicheskiye velichiny. Spravochnik / Pod. red. I.S. Grigoriyeva, Ye.Z. Meylikhova. Energoatomizdat, M. (1991). (in Russian).
- [26] K.A. Mkhoyan, A.W. Contryman, J. Silcox, D.A. Stewart, G. Eda, C. Mattevi, S. Miller, M. Chhowalla. Nano Lett. **9**, 3, 1058 (2009).
- [27] A.T. Smith, A.M. LaChance, S. Zeng, B. Liu, L. Sun. Nano Mater. Sci. **1**, 1, 31 (2019).
- [28] P.P. Brisebois, M. Siaj. J. Mater. Chem. C **8**, 5, 1517 (2020).
- [29] K.Z. Donato, H.L. Tan, V.S. Marangoni, M.V.S. Martins, P.R. Ng, M.C.F. Costa, P. Jain, S.J. Lee, G.K.W. Koon, R.K. Donato, A.H. Castro Neto. Sci. Rep. **13**, 1, 6064 (2023).
- [30] A.H. Castro Neto, F. Guinea, N.M.R. Peres, R.S. Novoselov, A.K. Geim. Rev. Mod. Phys. **81**, 1, 109 (2009).
- [31] T.O. Wehling, E. Sastoglu, C. Friedrich, A.I. Lichtenstein, M.I. Katsnelson, S. Blügel. Phys. Rev. Lett. **106**, 23, 236805 (2011).
- [32] T. Susaki, A. Makishima, H. Hosono. Phys. Rev. B **84**, 11, 115456 (2011).
- [33] Z. Zhong, P. Hansmann. Phys. Rev. B **93**, 23, 235116 (2016).
- [34] K. Cieslik, D. Wrana, M. Rogala, C. Rodenbücher, K. Szot, F. Krok. Crystals **13**, 7, 1052 (2023).
- [35] M.I. Dar, A.K. Chandiran, M. Grätzel, M.K. Nazeeruddin, S.A. Shivashankar. J. Mater. Chem. A **2**, 6, 1662 (2014).
- [36] Y.E. Tasisa, T.K. Sarma, R. Krishnaraj, S. Sarma. Res. Chem. **11**, 101850 (2024).
- [37] D. Niesner, T. Fauster. J. Phys.: Condens. Matter **26**, 39, 393001 (2014).
- [38] Y.-J. Yu, Y. Zhao, S. Ryu, L.E. Brus, K.S. Kim, P. Kim. Nano Lett. **9**, 10, 3430 (2009).
- [39] F. Bechstedt, R. Enderlein. Semiconductor Surfaces and Interfaces. De Gruyter (1989).
- [40] S.Yu. Davydov. Phys. Solid State **58**, 6, 1222 (2016).
- [41] J. Robertson. Eur. Phys. J. Appl. Phys. **28**, 3, 265 (2004).
- [42] G.M. Rignanese. J. Phys.: Condens. Matter **17**, 7, R357 (2005).
- [43] M.E. Levinshtein, S.L. Rumyantsev, M.S. Shur. Properties of Advanced Semiconductor Materials. Wiley, N.Y. (2001).
- [44] R. Bessler, U. Duerigh, E. Koren. Nanoscale Adv. **1**, 5, 1702 (2019).
- [45] X. Huang, T. Leng, T. Georgiou, J. Abraham, R.R. Nair, K.S. Novoselov, Z. Hu. Sci. Rep. **8**, 1, 43 (2018).
- [46] E. Prokhorov, Z. Barquera-Bibiano, A. Manzano-Ramírez, G. Luna-Barcenas, Y. Kovalenko, M.A. Hernández-Landa-verde, B.E.C. Reyes, J.H. Vargas. Mater. Res. Express **6**, 8, 085622 (2019).
- [47] K. Yim, Y. Yong, J. Lee, K. Lee, H.-H. Nahm, J. Yoo, C. Lee, C.S. Hwang, S. Han. NPG Asia Materials **7**, 6, e190 (2015).
- [48] C. Verdi, F. Caruso, F. Giustino. Nature Commun. **8**, 1, 15769 (2017).
- [49] T.J. Smart, T.A. Pham, Y. Ping, T. Ogitsu. Phys. Rev. Mater. **3**, 10, 102401(R) (2019).
- [50] L. Zhang, W. Chu, C. Zhao, Q. Zheng, O.V. Prezhdo, J. Zhao. J. Phys. Chem. Lett. **12**, 9, 2191 (2021).
- [51] S.Yu. Davydov. Semiconductors **52**, 2, 226 (2018).
- [52] S.Yu. Davydov. Semiconductors **52**, 3, 335 (2018).

*Translated by A.Akhtyamov*